

Hydration of the Yttrium(III) Ion in Aqueous Solution. An X-ray Diffraction and XAFS Structural Study

Patric Lindqvist-Reis,[†] Kathryn Lamble,[†] Sidhartha Pattanaik,[†] Ingmar Persson,^{*,‡} and Magnus Sandström^{*,†}

Department of Chemistry, Royal Institute of Technology, S-100 44 Stockholm, Sweden, and Department of Chemistry, Swedish University of Agricultural Sciences, P.O. Box 7015, S-750 07 Uppsala, Sweden

Received: June 23, 1999; In Final Form: October 5, 1999

The yttrium(III) ion is found by means of extended X-ray absorption fine-structure spectroscopy (EXAFS) and large angle X-ray scattering (LAXS) to be hydrated by eight water molecules in aqueous solution. The EXAFS data show a slightly asymmetric distribution of the Y–O bond distances with the centroid of the distribution at 2.368(5) Å. The width of the distribution implies a positional disorder of about 0.1 Å on top of the thermally induced variation in the Y–O bond distances. The aqueous solutions and the solid compound [Y(OH₂)₈]Cl₃·(15-crown-5), in which eight water oxygen atoms form a distorted bicapped trigonal prism around the hydrated yttrium(III) ion, show very similar near-edge and EXAFS spectra. For aqueous solutions the LAXS data give a mean Y–O bond distance of 2.365(5) Å and show the presence of a second hydration sphere consisting of approximately 16 oxygen atoms at a mean Y···O distance of 4.40(4) Å.

Introduction

The structure of the hydrated yttrium(III) ion varies considerably in its solid hydrates. Eight or nine are the most common coordination numbers,¹ but six-coordination has been proposed for the perchlorate salt.² In the eight-coordinated complexes the arrangement of the oxygen atoms has often been described as either a distorted square antiprism or a dodecahedron with a considerable spread in the Y–O bond distances. The usual geometry for nine-coordination is the tricapped trigonal prism, with two well-separated groups of Y–O bond distances. The average bond distance for eight-coordination is typically 2.35–2.38 Å; for nine-coordination, it is slightly longer. Figure 1 shows the spread in the individual Y–O bond distances in a selection of solid hydrates. The variations seem to depend both on packing effects and on the hydrogen bonding to the outer sphere. No eight-hydrated yttrium complex has been found in the solid state with all Y–O distances equal, which would correspond to the energetic minimum of eight electric dipoles in a square antiprism.³ For six-coordination the expected mean Y–O bond distance can be estimated to about 2.28 Å from the structure of yttrium(III) oxide.⁴

Yttrium(III) is similar in size and chemical behavior with the heavy lanthanide(III) ions.¹² The similarity in ionic radii has been utilized by Johansson et al. for isomorphous substitution in large angle X-ray scattering (LAXS) experiments to study the structure of the hydrated lanthanide(III) ions in aqueous solution.¹³ Difference curves with yttrium(III) solutions of the same molar concentrations were used to eliminate light atom interactions. Assuming regular eight-hydration of yttrium(III) it was concluded that not only erbium(III) and terbium(III) but also lanthanum(III) and samarium(III) were eight-hydrated, although differences in the H₂O–H₂O interactions in the first and second hydration spheres were found.^{13a} However, in aqueous solution considerable evidence shows a change in the hydration number from nine to eight with increasing atomic number in the middle of the series of the lanthanide(III) ions,

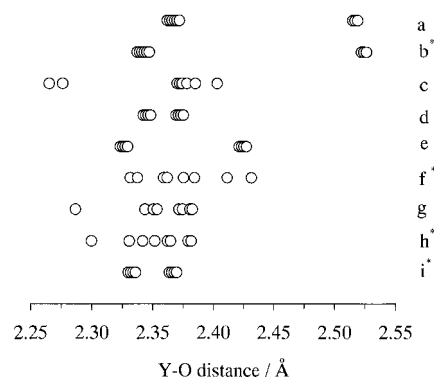


Figure 1. Individual Y–O bond distances obtained from X-ray diffraction of eight- and nine-coordinated crystalline hydrates: (a) [Y(OH₂)₉](EtOSO₂)₃, ref 5; (b) [Y(OH₂)₉](CF₃SO₃)₃, ref 6; (c) [Y(OH₂)₆-(OSMe₂)₂]Cl₃ (2 × 2.27 Å for Y–O(dmsO)), ref 7; (d) [Y(OH₂)₈]Tc₂-Cl₈·H₂O, ref 8; (e) [Y(OH₂)₈]Cl₃·2C₁₀H₈N₂, ref 9; (f) [Y(OH₂)₈]Cl₃·(15-crown-5), ref 10; (g) [Y(OH₂)₆(C₁₀H₇SO₃)]C₁₀H₇SO₃·3H₂O, ref 11; (h) [Y(OH₂)₆(C₇H₇SO₃)₂]C₇H₇SO₃·3H₂O, ref 11; (i) [(H₂O)₄Y(μ-OSO₂-CH₃)₂]CH₃SO₃_n, ref 7. Model compounds used for the EXAFS study are b, f, h, and i.

“the gadolinium break”.^{1,14} Both X-ray diffraction and extended X-ray absorption fine structure spectroscopy (EXAFS) have been used previously for structure studies of the hydrated yttrium(III) ion in very concentrated (≈ 2.7 M YX₃) aqueous halide (X = Cl, Br) solutions, for which no acid to prevent hydrolysis seems to have been added.^{15,16} The hydration number was assumed to be eight, and the mean Y–O distance was reported to be about 2.33 Å from EXAFS and 2.36 Å from the LAXS results.^{15,16} From a recent EXAFS study of YBr₃ solutions the mean Y–O distance 2.35 Å was reported to be independent of the yttrium concentration in the range 0.005–2.0 mol·dm⁻³.¹⁷ No inner-sphere halide ion pairing was found,¹⁷ consistent with the absence of halide complexes in aqueous solution,¹⁸ verified by Raman spectroscopy of yttrium(III) in concentrated halide solutions¹⁵ and also in solutions with a large excess of hydrochloric acid.⁷

In the present work yttrium K-edge X-ray absorption spectroscopy (XAS) has been combined with a LAXS study to obtain

[†] Royal Institute of Technology.

[‡] Swedish University of Agricultural Sciences.

more detailed information about the local structure around the hydrated yttrium(III) ion. The low-energy part of the XAS spectrum usually contains a significant amount of multiple scattering from the tightly bonded first shell of atoms, which can give information on the coordination geometry around the absorbing (central) atom. The high-energy EXAFS region provides direct information about the distance between the central atom and its nearest neighbors, in this case Y—O_I of the first hydration sphere. Both the EXAFS and LAXS techniques can give precise mean metal—oxygen bond distances, but not very accurate coordination numbers. In cases with large disorder in the first shell theoretical modeling of the multiple scattering, based on analyses of separate multiple scattering pathways, becomes difficult. However, qualitative comparisons between the XAS edge-structure of the unknown sample and of model compounds with similar structure, may give useful indications of the coordination geometry.

The EXAFS functions normally cover a larger range of the scattering variable than in LAXS because of the backscattering of the ejected photoelectron.¹⁹ This increases the resolution, which allows a better possibility of evaluating positional disorder and asymmetry in the distribution of the metal—oxygen distances in the first coordination sphere. Conversely, the contributions from highly damped long-range interactions, such as Y···O_{II} to the second shell, are weak in EXAFS and overlapped by multiple scattering within the first shell. Long-range interactions are better represented in the LAXS data for which multiple scattering is not a problem.^{19,20} However, for LAXS studies of hydrated metal ions the overlap of other distances for interactions not involving the metal ion makes it necessary to use concentrated solutions.

In the present study XAS spectra of the hydrated yttrium(III) ion in aqueous solution have been compared with those of four crystalline model compounds with eight or nine-coordination, to determine the probable coordination geometry. The width and asymmetry of the distribution of the Y—O bond distances was evaluated by means of the EXAFS functions. Structural parameters for the second hydration sphere of the hydrated yttrium(III) ion were obtained from the LAXS data.

The crystal structures of the four solid hydrates chosen as model compounds show different coordination figures and Y—O bond distance distributions (cf. Figure 1). For both the compounds [Y(OH₂)₈]Cl₃·(15-crown-5) (S1) and [Y(OH₂)₆(C₇H₇SO₃)₂]C₇H₇SO₃·3H₂O (S2) the arrangement of the eight-coordinated oxygen atoms can be described as a distorted bicapped trigonal prism with the central yttrium atom slightly displaced toward the capping oxygens (Figure S1). The arithmetic mean of the Y—O bond distances is 2.373 Å for S1 (range 2.32–2.43 Å, Figure 1f)¹⁰ and 2.352 Å for S2 (range 2.30–2.38 Å, Figure 1h), with a more symmetric distribution of the oxygen atoms around yttrium in S2.¹¹ The capping oxygen atoms give rise to the two longest Y—O distances in Figure 1f,h. The coordination figure in the polymeric compound ([Y(OH₂)₄Y(μ-O₂SOCH₃)₂](CH₃SO₃)₃)_n (S3) is a square antiprism, with the mean Y—O bond distance 2.350 Å (4 × H₂O at 2.332 Å and 4 × OSO₂CH₃ at 2.367 Å, Figure 1i). In [Y(OH₂)₉](CF₃SO₃)₃ (S4) nine water molecules surround yttrium in a tricapped trigonal prism, with six Y—O bond distances at 2.344 Å in the prism and three at 2.525 Å in the capping positions; see Figure 1b.⁶

Experimental Section

Sample Preparation. The concentrations and labels used for the solutions studied by X-ray absorption and LAXS are given

TABLE 1: Concentrations (mol·dm⁻³), Density (ρ), and Linear Absorption Coefficient (μ) of the Aqueous Solutions Used for X-ray Absorption and Large Angle Scattering Measurements

label/sample	[Y ³⁺]	[X ⁻]	[H ⁺]	[H ₂ O]	ρ/g cm ⁻³	μ/cm ⁻¹
L1 ^{a,b} /Y(ClO ₄) ₃ in HClO ₄	1.71	5.42	0.29	44.4	1.49	18.3
L2 ^a /Y(ClO ₄) ₃ in HClO ₄	1.14	3.61	0.19	48.3	1.33	12.6
L3 ^a /Y(ClO ₄) ₃ in HClO ₄	0.43	1.35	0.06	57.6	1.12	5.5
L4 ^b /YI ₃ in dil HI(aq)	0.99	3.06	0.10	50.1	1.39	24.6
L5 ^b /YI ₃ in conc HI(aq)	1.00	10.00	7.00	39.8	2.11	58.0

^a EXAFS. ^b LAXS.

in Table 1. The aqueous solutions L1–L3 were prepared by dissolving yttrium oxide in perchloric acid with stirring and heating, L4 by dissolving yttrium iodide (Aldrich) in dilute iodic acid, and L5 by dissolving yttrium oxide (Merck) in concentrated iodic acid. Crystals of the model compound S1 were prepared as described elsewhere,¹⁰ and crystals of S2–S4 were formed after slow evaporation of the corresponding solution. The yttrium content of all samples was determined by EDTA titration using xylenol orange as indicator.²¹ The anion content was determined by cation exchange (Dowex 50W–X8, H⁺ form), followed by standard acid–base titration. The solid compounds were analyzed by X-ray powder diffraction methods, which gave cell dimensions in good agreement with reported values.^{5,6,8–11} The densities of the solutions were measured with an Anton Paar DMA 35 densitometer, and the flotation technique was used for the solids.²²

EXAFS Data. The yttrium K-edge X-ray absorption experiments were performed at the Stanford Synchrotron Radiation Laboratory (SSRL) using the wiggler beam line 4-1, equipped with a Si[220] double crystal monochromator. SSRL operates at 3.0 GeV and a maximum current of 100 mA. The data collection was performed in transmission mode at ambient temperature, and higher order harmonics were reduced by detuning the second monochromator crystal to 50% of maximum intensity at the end of the scans. The solids were diluted with boron nitride to give an edge step of about one unit in the logarithmic intensity ratio. The solutions were kept in cells with thin glass windows (ca. 35 μm) and 1–5 mm Teflon or Viton spacers. The energy scale of the X-ray absorption spectra was calibrated by simultaneously scanning an yttrium foil and assigning the first inflection point of the yttrium metal K-edge to 17038.0 eV. For each sample three or four spectra were calibrated and averaged by means of the EXAFSPAK program package.²³

The EXAFS oscillations were obtained after performing standard procedures for preedge subtraction, normalization, and spline removal by means of the WinXAS software.²⁴ Calculated model functions using ab initio calculated phase and amplitude parameters obtained by the FEFF7 program were curve-fitted to the *k*³-weighted EXAFS data.²⁵ The EXAFS function was then Fourier transformed over the *k* range 2–16 Å⁻¹ without a window function. The asymmetry of the Y—O shell was modeled by *r*-space fitting using the cumulant expansion method, including third and fourth cumulants, which compensates for phase and amplitude shifts, respectively.^{26,27} The shift Δ*E*₀ in the threshold energy was then kept constant at the value refined for a symmetrical distribution (Table 2), and when the fourth cumulant was refined, the coordination number was fixed.

The input files to the FEFF7 program for the solid hydrates

TABLE 2: EXAFS Least-Squares *r*-Space Model Fitting of the First Hydration Shell of the Yttrium(III) Ion in Solid Hydrates and Aqueous Solution (Δr 1.11–2.44 Å, Uncorrected for Phase Shift, k^3 -Weighted Data)^a

sample/species	XRD ^b	N ^c	<i>d</i> /Å	$\sigma^2/\text{\AA}^2$	$C_3/\text{\AA}^3$	$C_4/\text{\AA}^4$	$\Delta E_0/\text{eV}$	res
Solid Hydrates								
S1/YO ₈	2.373 ^d	8	2.373(2)	0.0055(2)	0.00015(4)	−0.000017(4)	−3.3	5.8
bicapped trigonal prism		8	2.373(2)	0.0058(2)	0.00015(4)		−3.3	6.0
S2/YO ₈	2.352 ^d	8	2.365(2)	0.0059(2)		−0.000029(4)	−3.3(1)	7.2
bicapped trigonal prism		8	2.354(2)	0.0045(2)	0.00008(4)		−2.6	4.4
		8	2.354(2)	0.0053(2)	0.00006(4)		−2.6	5.7
		8	2.351(2)	0.0056(2)			−2.6(1)	5.7
S3/YO ₈	2.350 ^d	8	2.355(2)	0.0054(2)	0.00010(4)	−0.000002(4)	−2.8	5.7
square antiprism		8	2.355(2)	0.0058(2)	0.00010(4)		−2.8	6.0
		8	2.350(2)	0.0059(2)			−2.8(1)	5.9
S4/YO ₉	2.344	6	2.349(3)	0.0040(2)			−3.2(2)	5.4
tricapped prism	2.525	3	2.470(3)	0.0044(2)			−3.2(2)	5.4
S4/YO ₉	2.40 ^d	9	2.389(3)	0.0066(2)	0.00033(4)	0.000002(4)	−3.2	5.3
asymmetry model		9	2.389(3)	0.0066(2)	0.00033(4)		−3.2	5.3
		9	2.374(3)	0.0070(2)			−3.2	7.8
Aqueous Solution								
L1/Y ³⁺ (aq)		8	2.368(3)	0.0050(2)	0.00013(4)	−0.000027(4)	−3.3	4.7
		8.1(2)	2.367(3)	0.0059(2)	0.00013(4)		−3.3	5.5
		8.2(2)	2.361(3)	0.0062(2)			−3.3(2)	5.8
L2/Y ³⁺ (aq)		8	2.367(3)	0.0051(2)	0.00015(4)	−0.000025(4)	−3.2	5.2
		8.1(2)	2.367(3)	0.0059(2)	0.00015(4)		−3.2	5.7
		8.2(2)	2.360(3)	0.0060(2)			−3.2(2)	6.2
L3/Y ³⁺ (aq)		8	2.368(3)	0.0053(2)	0.00015(4)	−0.000020(4)	−3.6	5.2
		8.0(2)	2.368(3)	0.0059(2)	0.00015(4)		−3.6	5.7
		8.1(2)	2.361(3)	0.0062(2)			−3.6(2)	6.4

^a Parameters: Coordination Number (N), Y–O Bond Distance (*d*), Debye–Waller Factor (σ^2), Third (phase adjustment) Cumulant C_3 and Forth (amplitude adjustment) Cumulant C_4 for Asymmetric Distribution, Shift of Threshold Energy (ΔE_0) and Residual (Res). the Standard Deviations Are Estimated from the Noise Level in High *k* Data.²⁴ ^b From the crystal structure positions. ^c S_0^2 fixed at 0.89 derived from S1 and S2. ^d Arithmetic mean value in Å.

S1–S4 were compiled from the corresponding crystal structures to contain the Cartesian coordinates of each atom within a radius of 5 Å from the yttrium center. The phase and amplitude parameters calculated for S1 were used for the aqueous solutions, as also the amplitude reduction factor $S_0^2 = 0.89(3)$, obtained by refinements on S1 and S2 with the hydration number 8.

Large Angle X-ray Scattering. Mo K α ($\lambda = 0.7107$ Å) radiation was used in a θ – θ diffractometer of Bragg–Brentano type for LAXS measurements on the aqueous solutions.²⁸ Intensity data were collected at 450 discrete points for scattering angles in the range $1^\circ < \theta < 65^\circ$. This corresponds to a range of 0.3 – 16.0 Å^{−1} of the scattering variable $s = (4\pi \sin \theta)/\lambda$. Two scans, each accumulating 100 000 counts at every preset angle, were averaged, giving a statistical error of about 0.3% in the measured intensities. Details of the data collection and the analysis procedure, and the most important expressions used in the treatment of LAXS data, are given elsewhere.²⁹

Two models were considered for the hydrated yttrium ion, eight-coordination with a single mean Y–O distance, and nine-coordination in a tricapped trigonal prism with two shells of oxygen atoms for which the two Y–O distances were refined independently. The hydrated perchlorate ion was described with previously obtained structural parameters.²⁰ Treatment of the LAXS data was carried out using the KURVLR program,³⁰ and least-squares refinements of the structural parameters were done with the STEPLR program.³¹

Results and Discussion

X-ray Absorption Spectroscopy. In the following section the structure of the first hydration shell of the yttrium(III) ion in aqueous solution is discussed, based on comparisons between the X-ray absorption spectra of the solution L1 with the eight-hydrated crystalline solids S1 and S2 and the nine-hydrated S4.

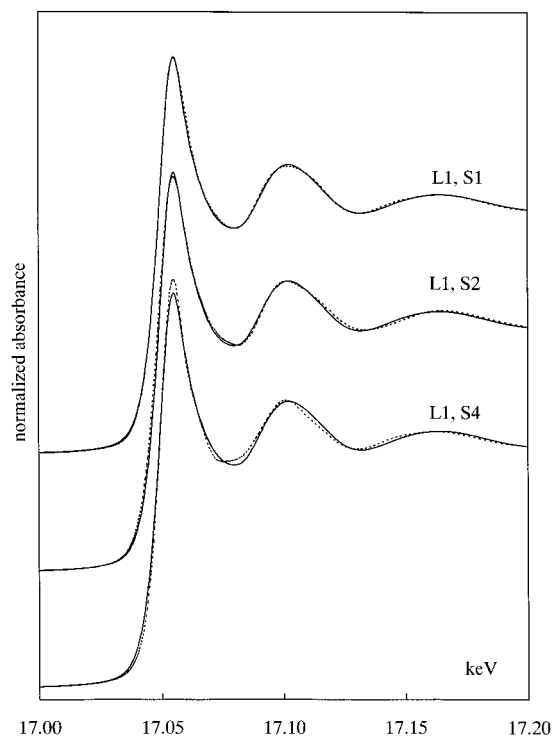


Figure 2. Yttrium K-edges and the XANES regions of the aqueous solution, L1 (solid line), compared to the solid hydrates S1, S2, and S4 (dashed lines). S1 = $[\text{Y}(\text{OH}_2)_8]\text{Cl}_3 \cdot (15\text{-crown-5})$, S2 = $[\text{Y}(\text{OH}_2)_6(\text{C}_7\text{H}_7\text{SO}_3)_2]\text{C}_7\text{H}_7\text{SO}_3 \cdot 3\text{H}_2\text{O}$, and S4 = $[\text{Y}(\text{OH}_2)_9](\text{CF}_3\text{SO}_3)_3$.

The edge structure (XANES) of the yttrium K-edge for the aqueous solution and the three solid hydrates is rather featureless; see Figure 2. A comparison of the edge positions for the aqueous and solid samples shows a small energy difference for sample S4 (-1.0 ± 0.5 eV). The intensity at the absorption maximum, around 17055 eV, of the eight-hydrated S1 and S2

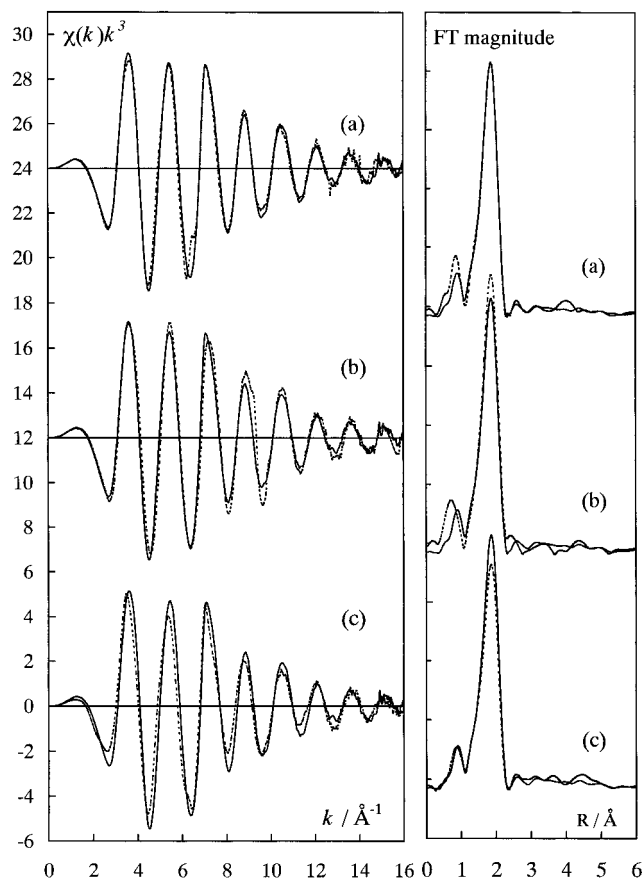


Figure 3. k^3 -weighted EXAFS data (left) and the corresponding Fourier transforms (right) of the aqueous yttrium(III) solution L1 (solid line) compared to the solid hydrates (dashed lines): (a) L1 and S1, (b) L1 and S2, (c) L1 and S4. Note the asymmetric wave shape at $k \approx 7 \text{\AA}^{-1}$ for L1, S1, and S4 (cf. ref 32).

is very similar to that of the aqueous solution, while the nonahydrate S4 differs somewhat. Differences between S4 and the aqueous solution are also seen in the region 17 060–17 100 eV, whereas the XANES features of the eight-hydrated solids S1 and S2 are very similar to those of the aqueous solution.

The k^3 -weighted EXAFS spectra of the yttrium(III) aqueous solution L1 and three of the crystalline yttrium hydrates are shown in Figure 3. The corresponding Fourier transforms (FTs, range $2 < k < 16 \text{\AA}^{-1}$) for S1, S2, and S4 in Figure 3 are almost featureless for r values above the Y–O₁ peak. This shows that the backscattering from the first coordination sphere is dominating in the FT range, with only minor contributions from multiple scattering within the first coordination shell and from backscattering from the second shell. Qualitative comparisons between the EXAFS spectra of the aqueous solution and the solid model compounds are then feasible in order to find similarities in their Y–O bond distances and distribution.

For the model compounds S2 and S4 the EXAFS spectra are slightly out of phase at lower k values in comparison with the aqueous solution, a positive and negative shift for S2 and S4, respectively. The magnitude of the FTs of S2 and S4 also differs from that of the aqueous solution, higher and lower, respectively; see Figure 3. However, it is evident from both the EXAFS spectra and the FTs that the mean Y–O distance and the Y–O bond distance distribution in the eight-hydrated model compound S1 and the aqueous solution L1 are very similar, indicating closely similar Y–O coordination.³²

To obtain structural parameters of the first hydration shell for the aqueous solutions and the hydrated salts, r -space fitting

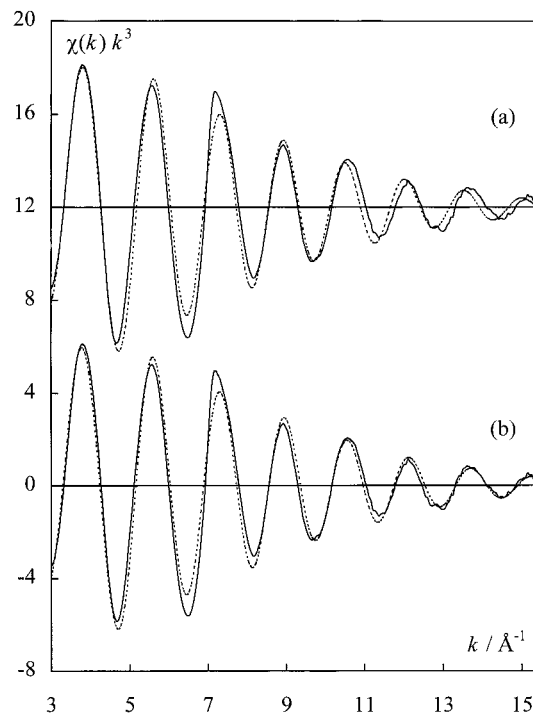


Figure 4. k^3 -weighted unfiltered EXAFS data of the aqueous yttrium(III) solution, L1 (solid lines) and the model function (dashed lines) of the Y–O shell obtained from least-squares refinement in r -space assuming (a) symmetric and (b) asymmetric distribution of Y–O contributions, the latter by introducing a third cumulant. See Table 2 for details.

was performed of only the Y–O₁ peak in the FT. This procedure avoids influence from the weak EXAFS oscillations mainly originating from various multiple scattering paths with longer r values. Asymmetry of the positional disorder around the yttrium(III) ion in each sample was accounted for by the cumulant expansion method. The mean values obtained for the Y–O bond distances of the model compounds (S1–S4) from the EXAFS data are very similar to the crystal structure values except for the weakly coordinated capping oxygen atoms in S4, which were shorter than the reported distance in the crystal structure; see Table 2. The best fit for the aqueous solutions L1–L3 was obtained with eight oxygen atoms around yttrium at the Y–O distance $2.368 \pm 0.005 \text{\AA}$. The uncertainty in the distance mainly originates from the estimated error in the threshold energy E_0 , about $\pm 0.3 \text{ eV}$. All structural parameters for the three solutions are very similar, showing no concentration dependence ($0.4\text{--}1.7 \text{ mol}\cdot\text{dm}^{-3}$).

The EXAFS functions of the model compounds display different degrees of asymmetry of the distribution of their Y–O distances. Curve-fitting in k -space with Debye–Waller factors corresponding to a symmetric (Gaussian) distribution reveals a phase shift at high k values ($k > 10 \text{\AA}^{-1}$) and also a displacement of the sine transform relative to the magnitude of the FT (Figure S2), which is an indication of asymmetry.²⁶ This is small for S2 and S3 but significant for S1, S4, and the aqueous solutions. However, by introducing a third cumulant, C_3 , to the EXAFS expression,²⁷ this phase difference disappears and the mean Y–O bond distance increases. For the aqueous solutions and the compound S1 the increase is about 0.007\AA , but smaller for the compounds S2 and S3; see Figure 4 and Table 2. For the model compounds the C_3 values were found to depend on the type of asymmetry. Two groups of distances, separated by Δr as in S4, give a higher value than a more even distribution of distances within the same Δr range (cf. S4 in Table 2). The

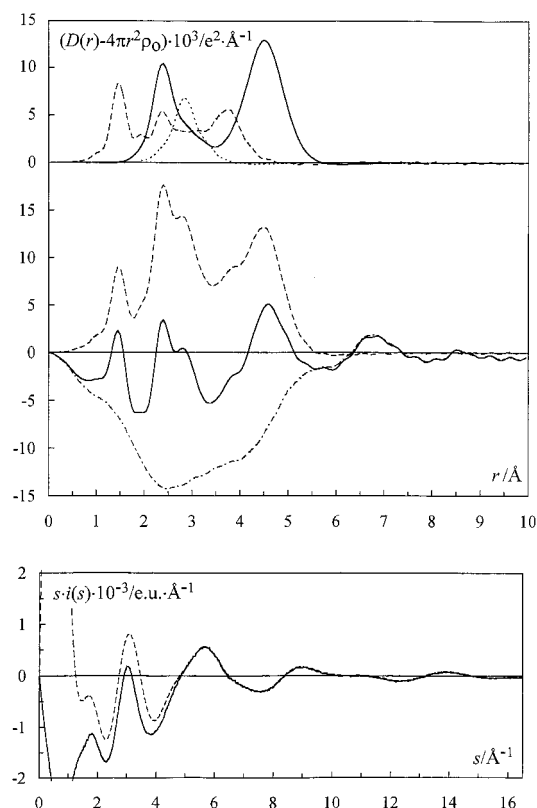


Figure 5. (Top) LAXS radial distribution curves for a 1.7 mol·dm⁻³ acidic aqueous solution of yttrium perchlorate (L1). (Upper part) separate model contributions: the eight-hydrated yttrium(III) ion (Table 2) with the first and second sphere (solid line), the hydrated perchlorate ion (dashed line), and O_w...O_w in the aqueous bulk (dotted line). (Middle) experimental RDF: $D(r) - 4\pi r^2 \rho_0$ (solid line); sum of model contributions (dashed line); difference (dash-dotted line). (Bottom) reduced LAXS intensity functions $si(s)$ (solid line); model $si_{calc}(s)$ (dashed line).

aqueous solutions and S1 have similar C_3 values as well as Debye–Waller parameters σ , indicating similar distributions of distances. For a symmetrical distribution the σ values correspond to root-mean-square deviations of 0.077 Å from the mean distance.

In a wide distribution of Y–O bond distances the shorter ones are expected to contribute more than the longer ones, to the outer part of the k -space EXAFS data, because of a longer period in the sinusoidal oscillations and a smaller Debye–Waller factor. The individual Y–O contributions will thus get different weights in different parts of the EXAFS spectrum. For solution L1 refinements of the Y–O interaction by increasing the lower limit k_{min} or reducing the upper cutoff k_{max} of the k range showed a large variation in the apparent mean distance, from 2.33 to 2.42 Å, respectively.

To test the significance of the proposed models a two-shell model of 6 and 3 oxygen atoms, respectively, was also tested for the first coordination sphere of L1. Refinement in r -space gave a slightly inferior fit for the Y–O distances 6×2.33 and 3×2.45 Å, i.e., slightly shorter than the values obtained for the solid nonhydrate S4, which has 6 + 3 hydration (Table 2). However, also for S4 the Y–O_{capping} distance (Table 2) from the EXAFS refinements is shorter than the value obtained from the crystal structure, 2.470(3) and 2.525 Å, respectively. A similar but more pronounced effect was also evident for the scandium triflate, [Sc(OH₂)₈](CF₃SO₃)₃, isomorphous with S4, in which one capping water molecule was found to be missing, causing a displacement of the metal ion toward the remaining capping oxygen atoms.⁷

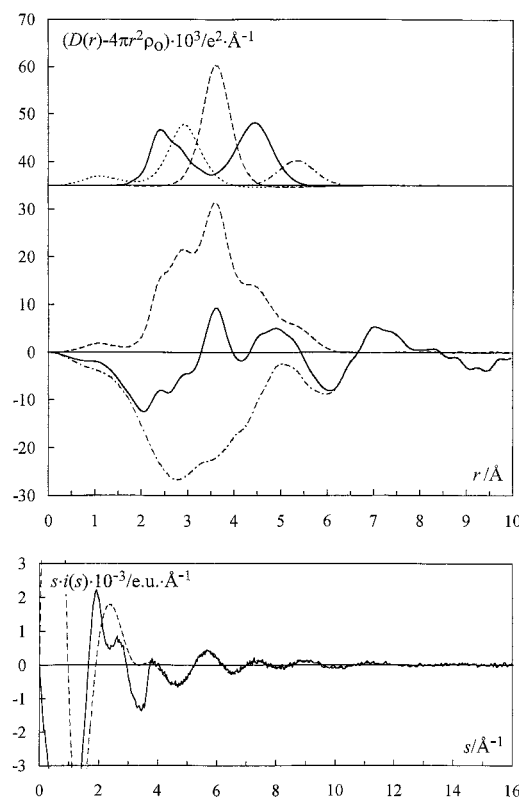


Figure 6. (Top) LAXS radial distribution curves for a 1.0 mol·dm⁻³ aqueous solution of yttrium iodide (L4). (Upper part) separate model contributions: the eight-hydrated yttrium ion with the first and second sphere (solid line), the hydrated iodide ion (dashed line), and O_w...O_w in the aqueous bulk (dotted line). (Middle) experimental RDF: $D(r) - 4\pi r^2 \rho_0$ (solid line); sum of model contributions (dashed line); difference (dash-dotted line). (Bottom) reduced LAXS intensity functions $si(s)$ (solid line); model $si_{calc}(s)$ (dashed line).

Large Angle X-ray Scattering. The radial distribution function (RDF) of the 1.7 mol·dm⁻³ acidic aqueous solution of yttrium(III) perchlorate (L1) shows major peaks at 1.45, 2.4, and 4.5 Å (Figure 5). The peaks at 2.4 and 4.5 Å correspond to the Y–O distances for two hydration spheres around the yttrium ion. The peak at 1.45 Å originates from the Cl–O bond distance in the hydrated perchlorate ion, which in tetrahedral symmetry has O...O distances of 2.37 Å. A rather broad peak at about 2.9 Å includes hydrogen-bonded O...O distances from the water structure, interactions within and between the first and second hydration sphere of the hydrated yttrium ion, and the hydrogen-bonded O...O distances around the hydrated perchlorate ion. To analyze the first sphere Y–O_i interaction at about 2.4 Å without overlap from perchlorate oxygen distances, a 1.0 mol·dm⁻³ yttrium(III) iodide (L4) solution was investigated (Figure 6). Besides the 2.4 and 4.5 Å peaks, a major peak occurs at 3.6 Å in the RDF of L4, which corresponds to the I...(H)–O distances of the hydrated iodide ion, and a broad peak appears at about 5 Å. As a check that there are no direct Y–I ion-pair contact distances, and also to get more reliable parameters for describing the interactions with the iodide ion, another very acidic yttrium(III) iodide solution was investigated (L5) in which the iodide concentration was increased to 10 mol·dm⁻³ (Figure S3). The RDF of this solution is dominated by two major peaks at 3.6 and 5.3 Å, corresponding to the I...(H)–O distances of the hydrated iodide ion and the Y...I second sphere distance. Minor peaks at 2.4 and 4.4 Å from the hydration spheres around the yttrium(III) ion were found, but no evidence for direct Y–I contacts.

TABLE 3: LAXS Least-Squares Model Fitting of the $\text{Y}(\text{ClO}_4)_3$ (L1) and YI_3 (L4, L5) Acidic Aqueous Solutions^a

	L1			L4			L5		
	<i>N</i>	<i>d</i>	<i>l</i>	<i>N</i>	<i>d</i>	<i>l</i>	<i>N</i>	<i>d</i>	<i>l</i>
Y–O _I	8	2.365(5)	0.128(3)	8	2.364(5)	0.124(3)	8	2.361(5)	0.083(3)
Y–O _{II}	16	4.41(4)	0.30(2)	14.9 ^b	4.40(4)	0.31(2)	12 ^b	4.37(4)	0.31(2)
O _I ···O _{II}	16	2.75(2)	0.13(2)	14.9 ^b	2.75(2)	0.11(2)	12 ^b	2.75	0.13
Cl–O	4	1.453(3)	0.066(4)						
O···O _w ^c	4	3.04(4)	0.21(2)						
Cl···O _w ^c	4	3.72(3)	0.21(2)						
O _w ···O _w ^d	2	2.89(2)	0.20(1)	2	2.89(1)	0.20(1)			
Y···I				1.1 ^b	5.32	0.22	4 ^b	5.32(2)	0.22(2)
I···O _w ^c				6	3.585(4)	0.21(1)	6	3.551(5)	0.21(1)
O _w ···O _w ^d							1.2	3.05(5)	0.25(3)

^a Parameters: Coordination Number *N*, Distance *d*/Å, and Disorder Parameter, *l* ($= 2\sigma$)/Å, for Refined Parameters Estimated Standard Deviations Are Given within Brackets. ^b From stoichiometric ratio (see text). ^c Water hydrogen bonded to perchlorate or iodide, ref 20. ^d Accounts for bulk water structure or water surrounding the iodide and yttrium ions.

The data analysis gave the best fit for an eight-coordinated model of the hydrated yttrium(III) ion with a mean Y–O bond distance of 2.365(5) Å both for L1 and L4, Table 3 (cf. Figure S4). The second hydration sphere was found to contain approximately sixteen oxygen atoms at a mean Y···O_{II} distance of 4.40(4) Å. The displacement factor, *l* (the root-mean-square variation in the Y–O bond distance, $l = 2\sigma$ in EXAFS) is 0.13(1) Å for the first sphere and 0.31(2) Å for the second sphere, the former close to the corresponding EXAFS value $2\sigma = 0.15$ (1) Å. The effective range of the scattering variable is much smaller for the model fitting of the LAXS data, with an *s*-range of 5 to 16 Å^{−1}, than the corresponding *k*-space range for the EXAFS data, 2 to 16 Å^{−1}, considering that *s* corresponds to 2*k* due to the backscattering process in EXAFS. Because of the resulting lower resolution in the LAXS data, no asymmetry can be detected in the first coordination sphere.

The hexahydrated chromium(III) and gallium(III) ions (M–O_I 1.96 Å) have much smaller displacement parameters with *l* values about 0.05 and 0.18 Å for their first and second spheres, respectively.²⁰ Also the larger hexahydrated indium(III) ion (In–O_I 2.13 Å) has relatively small *l* values, 0.087(4) and 0.23(1) Å for the first and second hydration spheres, respectively.²⁰ This comparison shows that the distribution of the Y–O distances is wider than that expected from thermal displacements alone. Assuming that the total bond length variation for symmetrical displacements is given by $l = \sqrt{(l_{\text{thermal}})^2 + (l_{\text{disorder}})^2}$, the contribution from positional disorder, *l*_{disorder}, is estimated to be about 0.10 Å (for *l*_{thermal} ≈ 0.08 Å), thus giving *l* ≈ 0.13 Å as in Table 3. This is of similar magnitude to the variation of the mean Y–O distance, from 2.33 to 2.42 Å, obtained from the EXAFS data in different *k* ranges (see above).

A test of the tricapped trigonal prismatic model for nine oxygen atoms around yttrium(III) gave a less good fit around $s = 5$ Å^{−1}, even though the number of parameters is larger (Figure S2). The final structural parameters including the hydrated yttrium(III), perchlorate, or iodide ions and the aqueous bulk are given in Table 3, while the corresponding fits are shown in Figures 5 and 6.

For the LAXS study of the perchlorate solution L1 a high yttrium concentration was chosen (Table 1) in order to distinguish the Y–O bonds from other interactions, e.g., the hydrogen-bonded O···O interactions. However, high salt concentrations may lead to solvent-shared ion-pair formation, especially around highly charged cations, which can influence the hydration structure in the second shell. The concentration data in Table 1 show that for solution L1 there would be on average $30.7/5.42 = 5.7$ water molecules per perchlorate ion outside the $\text{Y}(\text{H}_2\text{O})_8^{3+}$ complexes. Thus, from the stoichiometric

ratio about three of the 16 hydrogen-bonded oxygen atoms in the second hydration sphere are expected to be perchlorate oxygens, which is consistent with a weak shoulder in the RDF at about 5 Å from Y···Cl interactions (Figure 5). For the yttrium(III) iodide solutions L4 and L5 similar estimates give about one and four iodide ions in the second shell, respectively. For solution L5 it was possible to refine the solvent-shared ion-pair Y···I distance to 5.32(2) Å (Table 3). The results of the model fitting are consistent with about 16 hydrogen-bonded atoms in the second shell for each yttrium(III) ion, for the more dilute perchlorate and iodide solutions (Table 3 and Figure S2).

Conclusions

The hydrated yttrium(III) ion is eight-coordinated in aqueous solution with the Y–O bond distances centered around 2.37 Å. The EXAFS data, which have a higher spatial resolution than LAXS, show a slightly asymmetric distribution of the Y–O bonds. Thus, the mean value, or the centroid of the distribution,²⁶ becomes slightly dependent on the technique used since the weighting of the individual contributions is different. The introduction of a third cumulant in the EXAFS expression to model the asymmetry from the individual Y–O bond distances increased the mean Y–O distance by almost 0.01 Å as compared to the symmetric Gaussian distribution model. The contribution of positional disorder increasing the width of the distribution of Y–O bond distances on top of the thermal displacements is estimated to be at least 0.1 Å, similar to that found in the distorted bicapped trigonal prism of water molecules around the yttrium(III) ion in the solid $[\text{Y}(\text{OH}_2)_8]\text{Cl}_3 \cdot (15\text{-crown-5})$. Also, the XANES and EXAFS spectra are very similar for the solutions and the eight-hydrated solids with this coordination figure. No concentration dependence of the coordination was found for the relatively concentrated solutions studied (0.43–1.71 mol dm^{−3}). A second hydration sphere is formed with a mean Y···O distance of 4.40(4) Å, and with solvent-shared ion pairs of perchlorate or iodide ions in approximately the expected stoichiometric ratio. No contact ion-pairing was found, not even in a 10 mol·dm^{−3} iodide solution for which the Y···I distance of 5.32(2) Å was obtained for the solvent-shared ion pair.

Acknowledgment. We gratefully acknowledge the Swedish Natural Science Research Council for financial support and the Stanford Synchrotron Radiation Laboratory (SSRL) for allocation of beam-time and laboratory facilities. SSRL is operated by the Department of Energy, Office of Basic Energy Sciences. The SSRL Biotechnology Program is supported by the National Institutes of Health, National Center for Research Resources, Biomedical Technology Program, and by the Department of Energy, Office of Biological and Environmental Research.

Supporting Information Available: Figure S1 shows the bicapped trigonal coordination polyhedra of the model compounds $[\text{Y}(\text{OH}_2)_8]\text{Cl}_3 \cdot (15\text{-crown-5})$ (denoted S1) and $[\text{Y}(\text{OH}_2)_6(\text{C}_7\text{H}_7\text{SO}_3)_2]\text{C}_7\text{H}_7\text{SO}_3 \cdot 3\text{H}_2\text{O}$ (S2). Figure S2 displays the sine and magnitude transforms of the aqueous solution L1 (corresponding to the EXAFS functions in Figure 4). Figure S3 shows the intensity data and the Fourier transformed RDFs and model functions from the LAXS study of an aqueous yttrium iodide solution (L5) with high iodide concentration (cf. Table 3). Figure S4 shows the model fitting to the LAXS data of solution L1 (cf. Figure 5) assuming a nine-coordinated yttrium(III) aqua ion with tricapped trigonal prism geometry. This information is available free of charge via the Internet at <http://pubs.acs.org>.

References and Notes

- Richens, D. T. *The Chemistry of Aqua Ions*; Wiley: Chichester, U.K., 1997; Chapter 3.
- Glaser, J.; Johansson, G. *Acta Chem. Scand., Ser. A* **1981**, *35*, 639.
- Kowall, Th.; Foglia, F.; Helm, L.; Merbach, A. E. *J. Phys. Chem.* **1995**, *99*, 13078.
- Faucher, M. *Acta Crystallogr., Sect. B* **1980**, *36*, 3209.
- Broach, R.; Williams, J.; Felcher, G.; Hinks, D. *Acta Crystallogr. Sect. B* **1979**, *35*, 2317.
- Harrowfield, J. M.; Kepert, D. L.; Patrick, J. M.; White, A. H. *Aust. J. Chem.* **1983**, *36*, 483.
- Lindqvist-Reis, P.; Eriksson, L.; Sandström, M.; Persson, I.; Lidin, S.; Kristiansson, O.; Pattanaik, S. Unpublished data.
- Cotton, F. A.; Davison, A.; Day, V. W.; Fredrich, M. F.; Orvig, C.; Swanson, R. *Inorg. Chem.* **1982**, *21*, 1211.
- Bukowska-Strzyewska, M.; Tosik, A. *Acta Crystallogr., Sect. B* **1982**, *38*, 950.
- Rogers, R. D.; Kurihara, L. K. *Inorg. Chim. Acta* **1986**, *116*, 171; **1987**, *129*, 277.
- Ohki, Y.; Suzuki, Y.; Takeuchi, T.; Ouchi, A. *Bull. Chem. Soc. Jpn.* **1988**, *61*, 1, 393.
- Shannon, R. D. *Acta Crystallogr. Ser. A* **1976**, *32*, 751.
- Johansson, G.; Wakita, H. *Inorg. Chem.* **1985**, *24*, 3047. (b) Johansson, G.; Yokoyama, H. *Inorg. Chem.* **1990**, *29*, 2460.
- Yamaguchi, T.; Nomura, M.; Wakita, H.; Ohtaki, H. *J. Chem. Phys.* **1988**, *89*, 5153.
- de Barros Marques, M. I.; Alves Marques, M.; Resina Rodrigues, J. M. *J. Phys. Condens. Matter* **1992**, *4*, 7679.
- Cabaço, M. I.; Alves Marques, M.; de Barros Marques, M. I.; Bushnell-Wye, G.; Costa, M. M.; de Almeida, M. J.; Andrade, L. C. *J. Phys. Condens. Matter* **1995**, *7*, 7409.
- Díaz-Moreno, S. Estudio de la Estructura de Complejos Metálicos en Disolución mediante Espectroscopías de Absorción de Rayos X. Ph.D. Thesis, University of Sevilla, Spain, 1998; pp 139–174.
- Sillén, L. G.; Martell, A. E. *Stability Constants of Metal Ion Complexes*; Special Publs. 17 and 25; Chemical Society: London, 1964 and 1971. Högfeldt, E. *Stability Constants of Metal Ion Complexes, Part A*; Inorganic Ligands, No. 21; Pergamon Press: Oxford, U.K., 1982.
- Persson, I.; Sandström, M.; Yokoyama, H.; Chaudhry, M. Z. *Naturforsch.* **1995**, *50a*, 21.
- Lindqvist-Reis, P.; Muñoz-Páez, A.; Díaz-Moreno, S.; Pattanaik, S.; Persson, I.; Sandström, M. *Inorg. Chem.* **1998**, *37*, 6675.
- Schwarzenbach, G.; Flaschka, H. *Die Komplexometrische Titration*; Ferdinand Enke: Stuttgart, 1965.
- International Tables for Crystallography*, Vol. C; Kluwer Academic Publisher: Dordrecht, The Netherlands, 1995; p 142.
- George, G. N.; Pickering, I. J. EXAFSPAK—A Suite of Computer Programs for Analysis of X-ray Absorption Spectra; SSRL: Stanford, CA, 1993.
- Ressler, T. *J. Synchrotron Radiation* **1998**, *5*, 118.
- Zabinsky, S. I.; Rehr, J. J.; Ankudinov, A.; Albers, R. C.; Eller, M. J. FEFF code for ab initio calculations of XAFS. *Phys. Rev. B* **1995**, *52*, 2995. Ankudinov, A. Ph.D. Thesis, University of Washington, 1996.
- Crozier, E. D.; Rehr, J. J.; Ingalls, R. *X-ray Absorption, Principles, Applications, Techniques of EXAFS, SEXAFS, and XANES*; Koningsberger, D. C., Prins, R., Eds.; Wiley-Interscience: New York, 1988; Chapter 9.
- Bunker, G. *Nucl. Instrum. Methods* **1983**, *207*, 437.
- Klug, H. P.; Alexander, L. E. *X-ray Diffraction Procedures for Polycrystalline and Amorphous Materials*; Wiley: New York, 1974; Chapter 5.
- Stålhandske, C. M. V.; Persson, I.; Sandström, M.; Kamienska-Piotrowicz, E. *Inorg. Chem.* **1997**, *36*, 3174 and references therein.
- Johansson, G.; Sandström, M. *Chem. Scr.* **1973**, *4*, 195.
- Molund, M.; Persson, I. *Chem. Scr.* **1985**, *25*, 197.
- The EXAFS function of the aqueous solutions and the solids $[\text{Y}(\text{OH}_2)_8]\text{Cl}_3 \cdot (15\text{-crown-5})$ and $[\text{Y}(\text{OH}_2)_6](\text{CF}_3\text{SO}_3)_3$ has a somewhat asymmetric wave shape at $k \approx 7 \text{ \AA}^{-1}$. A similar feature was observed in the EXAFS spectra of the hydrated gadolinium(III) ion (S. Bénazeth et al. *Inorg. Chem.* **1998**, *37*, 3667). This feature is probably due to an electronic transition of the same kind as previously observed in the EXAFS spectra of strontium and barium; see ref 17 and: D'Angelo, P.; Nolting, H.-F.; Pavel, N. V. *Phys. Rev. A* **1996**, *53*, 798. And for lanthanum: Solera, J. A.; García, J.; Proietti, M. G. *Phys. Rev. B* **1995**, *51*, 2678.